Ab initio X-ray Absorption Spectroscopy Study of the Solvation Structure of Yttrium (III) in Dimethyl Sulfoxide

Sofía Díaz-Moreno*,† and Jesús Chaboy‡

Diamond Light Source Ltd, Harwell Science and Innovation Campus, Didcot, Oxfordshire, OX11 0DE, U.K., and Instituto de Ciencia de Materiales de Aragón, CSIC-Universidad de Zaragoza, 50009 Zaragoza, Spain.

Received: October 29, 2008; Revised Manuscript Received: January 11, 2009

The solvation structure of yttrium (III) in dimethyl sulfoxide has been determined by studying both the extended X-ray absorption fine structure (EXAFS) and the X-ray absorption near edge structure (XANES) regions of the Y K-edge absorption spectra. Although the EXAFS technique provides accurate information about the next neighbors coordination distances, no unambiguous determination of the coordination polyhedron is obtained. This failure is counteracted by the study of the near-edge part of the absorption spectrum (XANES) because of its high sensitivity to the bonding geometry. We have performed an extensive and systematic ab initio computation of the Y K-edge XANES spectrum of yttrium (III) in dimethyl sulfoxide within the multiple-scattering framework. The comparison between the experimental data and the theoretical calculations has demonstrated that the solvation sphere of the yttrium cation is best modeled by eight dimethyl sulfoxide molecules each oriented to give an Y−O−S angle close to 130°.

Introduction

The solvation structure of the yttrium (III) cation in different solvents has been a subject of controversy for several decades. This problem is mainly due to the fact that, in contrast with other trivalent cations, yttrium (III) can be found in numerous different coordination environments in crystalline solids. It is not surprising to find crystalline compounds where six ligands are surrounding the cation, forming a perfect octahedron, as is the case of YSCN or YDMF solvated compounds,[1,2] but it is equally possible to find other coordination environments in the solid state, such as nine or eight.[3−7] The difficulty of determining the solvation structure of Y(III) in solution extends even to the determination of the hydration structure of this cation, which only very recently has been solved.[8]

The case of the solvation structure of the cation when the nitrate salt of the dimethyl sulfoxide solvate, $[Y(DMSO)_3](NO_3)_3$, is dissolved in dry DMSO is another example in need of clarification. DMSO is a widely used solvent employed in a large variety of chemical reactions, as it dissolves both polar and nonpolar compounds, and it is soluble in water and in most organic solvents. Despite the fact that a wide range of techniques such as IR spectroscopy,[9] X-ray diffraction,[10,11] and X-ray absorption spectroscopy[11] have been used to determine the solvate structure, no consensus has yet been reached. To date, no unambiguous solution has been found, and many different environments have been proposed. Therefore, a short-range-order technique such as X-ray absorption spectroscopy (XAS) may be a sound tool to determine the solvation structure of Yttrium (III) in DMSO by directly probing the local atomic structure.

X-ray absorption spectroscopy (XAS) has proven to be an outstanding structural tool for studying the local environment around a selected atomic species in a great variety of systems.[12] At present, reliable structural parameters are commonly derived from the analysis of the extended X-ray absorption fine structure (EXAFS) region of the spectrum. However, the accuracy of the structural determinations obtained by EXAFS can in several cases be inconclusive due to the well-known limitations of the EXAFS fitting methodology to determine coordination numbers and polyhedral environments.[8] In these cases, the study of XANES can provide useful complementary information, as the near-edge region of the spectrum is very sensitive to the geometrical details of the absorbing site (overall symmetry, distances, and bond angles). Despite the higher sensitivity of XANES to the bonding geometry, few structural determinations have been reported to date in which the analysis of this region of the X-ray absorption spectrum has been used. The main reason being that the ab initio computation of XANES spectra is not so straightforward as for EXAFS, as XANES computation requires sophisticated simulation tools.

In this work we have undertaken a study of the solvation structure of yttrium(III) prepared by dissolving the nitrate salt of the solvate in anhydrous dimethyl sulfoxide by combining both EXAFS and XANES techniques. The EXAFS determination of the coordination numbers in this system is limited in its ability to an accuracy no better than 20%. Furthermore, the general sensitivity of this method to the geometric form of the local coordination polyhedra is inconclusive. Consequently, we have performed a detailed ab initio study of the Y K-edge XANES spectrum of this solution within the multiple-scattering framework. Careful consideration is needed for the selection of the optimum parameters for the XANES computations. To do this, calculations have been performed for different reference compounds of known structure, and special attention has been paid to investigate the improvements obtained by using different treatments of the exchange-correlation part of the final state potential, modeled to obtain the best agreement both in energy and intensity, between the experimental and theoretical XANES spectra. These results have been transferred to the analysis of the solution sample, and several possible coordination environments and conformations of the DMSO molecule have been

* To whom correspondence should be addressed. E-mail: sofia.diaz-moreno@diamond.ac.uk.
† Diamond Light Source Ltd.
‡ CSIC-Universidad de Zaragoza.

10.1021/jp809575g CCC: $40.75
Published on Web 02/25/2009

investigated. Our results indicate that the solvation sphere of the yttrium cation is best modeled by eight DMSO molecules oriented such that the Y−O−S angle is close to 130°.

Experimental and Computational Methods

X-ray absorption experiments at the yttrium K-edge were carried out on (i) solid enneahydrated yttrium(iii) trifluoromethanesulfonate $[Y(H_2O)_9][CF_3SO_3]_3$ (hereafter abbreviated as yttrium(III) triflate); (ii) solid yttrium dioxide (Y_2O_3); (iii) a 0.5 M solution of tetra-n-butylammonium hexakis(thiocyanato-N)yttrate(III), $[Bu_4N]_3[Y(NCS)_6]$ in acetonitrile (henceforth YNCS), and (iv) solid tris(dimethylsulfoxide) yttrium(III) nitrate (hereafter, YDMSO), and its 0.5 M solution in dry DMSO.

Sample Preparation. Yttrium(III) triflate was prepared following the method proposed by Harrowfield et al.[3] The solid was used as a model compound against which comparisons could be made since its hydration structure is well-known.

Yttrium dioxide was used as commercially available (Aldrich).

YNCS was synthesized by deposition in crystalline form from a solution of YCl_3 and tetra-n-butylammonium thiocyanate in a molar ratio 1:10 in ethanol.[1] The 0.5 M solution was prepared by dissolving the required amount of the synthesized solid in dry acetonitrile.

YDMSO was synthetized following the method by Ramalingam.[9] Excess DMSO (3 mL) was added dropwise with stirring to a solution of yttrium nitrate pentahydrate (∼1 mol) in methanol (15 mL). The solvent was evaporated under reduced pressure over P_2O_5, and a precipitate of the complex was obtained in good yield. The precipitate was filtered, washed with benzene, dried over P_2O_5, and recrystallized from methanol. The 0.5 M solution was prepared by dissolving the required amount of the nitrated salt in dry DMSO.

XAS Measurements. Yttrium K-edge XAS spectra were recorded at the BL10B station of the Photon Factory (National Laboratory for High Energy Physics KEK, Japan). The storage ring was operated at 2.5 GeV, with a stored current of 300 mA. Measurements were performed at room temperature in the transmission mode with a Si(311) channel-cut monochromator. Ion chambers, filled with a He/Ar gas mixture and optimized to absorb 20% of the beam intensity in I_0 and 80% in It, were used as detectors. The solid compound yttrium(III) triflate was measured in a sample holder covered by kapton and placed in a hermetically sealed plastic bag, as this sample is very hygroscopic. The nonhygroscopic samples were measured in air. All liquid samples were measured in a specially designed cell, allowing for variable path lengths.[13]

EXAFS Data Analysis. The background corrections required to obtain the EXAFS functions $\chi(k)$ from the measured X-ray absorption spectra were performed using the Athena code.[14] E_0 was defined as the maximum of the first derivative of the absorption edge. To analyze the EXAFS spectra of the solutions, the theoretical phases and amplitudes were calculated by using the FEFF 6.00 code.[15] The fit to the experimental data was performed using the Artemis program (version 0.8.012).[16]

Computational Methods. The computation of the Y K-edge XANES spectra was performed by using the multiple-scattering code CONTINUUM[17] based on the one-electron full-multiple-scattering theory.[18,19] A complete description of both the theoretical basis and the calculation procedures can be found elsewhere.[20,21] In the following, only a brief summary of the computational details relevant to our particular case is given.

The potential for the different atomic clusters was approximated by a set of spherically averaged muffin-tin (MT) potentials built by following the standard Mattheis' prescription.[22] The MT radii were determined following the Norman criterion and by imposing a 10% overlapping factor.[23] The Coulomb part of each atomic potential was generated using charge densities for neutral atoms obtained from the tabulated atomic wave functions by Clementi and Roetti.[24] Three different approximations were performed for the excited-state potential: (i) the same potential as for the ground-state was used; (ii) relaxed $Z + 1$ rule, that is,, where the orbitals of Y are considered to relax after the creation of the 1s core-hole so as to resemble to those of Zr ($Z + 1$) neutral atom. Effectively, we substitute the atomic orbitals of Y with those of Zr imposing a 1s core-hole and removing an additional electron from the valence band; (iii) in the former case only relaxation is taken into account, thereby neglecting the tendency of the valence electrons to screen the hole under the core-hole attraction. This effect can be incorporated in the calculations by considering an extra electron filling the last occupied atomic orbital in the so-called screened and relaxed $Z + 1$ approximation. During the present calculations the three methods have been tested. We have found the screened and relaxed $Z + 1$ option leads to the best performance into simulate the experimental Y K-edge absorption spectra.

Different choices have been tested for the exchange and correlation part of the final state potential, including the energy-dependent Hedin−Lundqvist (HL) complex potential and the energy-dependent Dirac−Hara (DH) exchange potential. The calculated theoretical spectra have been further convoluted with a Lorentzian shape function ($\Gamma = 4$ eV) to account for the core-hole lifetime[25] and the experimental resolution. Finally, the maximum angular momentum quantum number used in the calculations was $l_{max} = 4$, having verified that no changes are induced in the simulated spectra in the energy interval of interest, up to ≃60 eV above the edge when further increasing the maximum l. For the comparisons, the experimental XANES spectra were normalized, after background subtraction, at high energy (∼100 eV above the edge) to eliminate thickness dependence.

Results and Discussion

The experimental EXAFS signal and the modulus of the associated Fourier transform of the 0.5 M solution of the tetrakis(dimethylsulfoxide)yttrium (III) nitrate in DMSO are shown in Figure 1. Three different coordination polyhedra were considered for the analysis of the EXAFS functions: (i) six DMSO molecules forming a perfect octahedral arrangement[9] (hereafter, the C6 model); (ii) eight DMSO molecules forming a distorted square antiprism[11] (hereafter C8); and (iii) nine DMSO molecules forming a tricapped trigonal prism[3] (hereafter, C9). The best fits obtained using these structural models are included in Figure 1. In all cases, the EXAFS analysis was carried out using two coordination spheres: the first one formed by coordinating oxygen atoms and the second by sulfur atoms. In the case of both C6 and C8 models, six fitting parameters were used in the fit, corresponding to the coordination distances for the oxygen and the sulfur shells, r_{Y-O} and r_{Y-S} respectively, the Debye−Waller factors for the two spheres, σ^2_{Y-O} and σ^2_{Y-S}, the inner potential correction for the system, ΔE_0, and the many-body amplitude reduction factor S_0^2. In the case of the C9 model, the number of fitting parameters used in the analysis was eight, as two different r_{Y-O} and r_{Y-S} interatomic distances have to be considered. The coordination numbers for the oxygen and the sulfur atoms were kept fixed during the fitting procedure in all the cases. As shown in Figure 1, although the quality of the fit

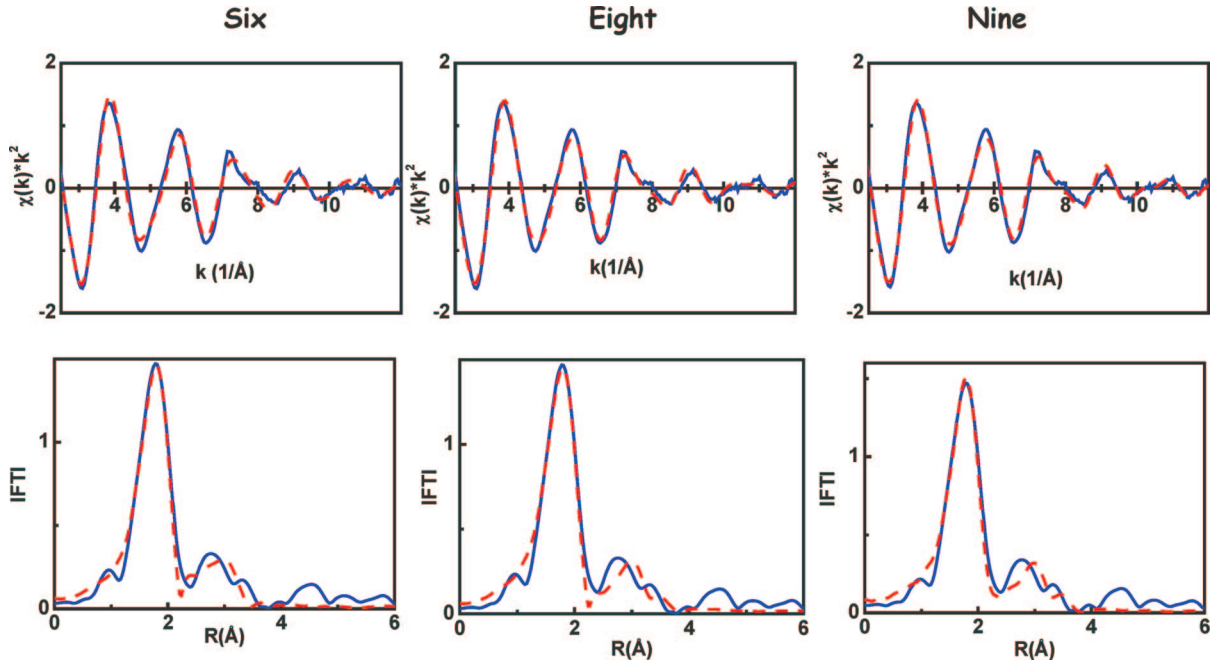

Figure 1. Comparison of the experimental Y K-edge k^2-weighted EXAFS spectrum of a 0.5m solution of yttrium (III) in DMSO (blue, solid line) and the EXAFS signal of the first solvation shell (red, dash) calculated for three different coordination polyhedra (See text for details). In the lower panel, the comparison of the modulus of the Fourier transform of the experimental k^2-EXAFS spectrum at the Y K-edge (blue, solid line) and the fitting results (red, dash) is shown.

TABLE 1: Best Fit Parameters Obtained from the Analysis of the Experimental EXAFS Spectrum of the Y(III) in DMSO[a]

model	N_{Coord} fixed	r_{Y-O} (Å)	σ^2_{Y-O} (Å^2)	r_{Y-S} (Å)	σ^2_{Y-S} (Å^2)	ΔE_0 (eV)	S_0^2	R
C6	6	2.36 ± 0.01	0.008 ± 0.002	3.56 ± 0.03	0.011 ± 0.005	4.0 ± 1.2	1.4 ± 0.2	0.01
C8	8	2.36 ± 0.01	0.008 ± 0.002	3.56 ± 0.03	0.009 ± 0.004	5.0 ± 1.2	1.0 ± 0.1	0.008
C9	3	2.34 ± 0.01	0.004 ± 0.002	3.54 ± 0.02	0.008 ± 0.004	5.5 ± 1.4	1.0 ± 0.1	0.006
	6	2.48 ± 0.04		3.68 ± 0.06				

[a] $\Delta k = 2.5-12$ Å^{-1}; $\Delta R = 1-3.6$ Å; N_{Coord}, coordination number; d, interatomic distance; σ^2, Debye-Waller factor; ΔE_0, inner potential correction; S_0^2, many-body amplitude reduction factor; R, reliability factor.[14,16]

is similar for the three models, coordination six is the least probable due to the high S_0^2 value (1.4 ± 0.2) that has to be used to compensate for the low coordination number used in the fit. The parameters obtained for the best fit to the experimental spectrum with the three different model polyhedra are summarized in Table 1.

From the analysis above it is clear that EXAFS structural determination is of limited value in this case, as the analysis is not conclusive regarding the different coordination polyhedra of the solvent structure of Yttrium (III) in DMSO. To proceed, we have thus performed an Y K-edge XANES study by comparing the experimental XANES spectrum to theoretical computations. In order to evaluate the results in a self-consistent way, we have performed the calculations for different reference compounds of known structure and for the Yttrium (III) solution in DMSO using the same conditions. Consequently, throughout the analysis, special attention has been paid to optimize several computational details intending to furnish the best agreement, both in energy and intensity, between the experimental and theoretical XANES spectral features.

We have selected both Yttrium(III) triflate and Yttrium oxide, Y_2O_3, as the reference compounds for optimizing the computational details. Initially, we have determined the minimum cluster size needed to reproduce all the experimental spectral features. This was achieved by performing ab initio computations of the Y K-edge in the case of Yttrium(III) triflate for different cluster sizes around the photoabsorbing Y atom. Starting from the simplest octahedral Y−O arrangement, r_{Y-O} = 2.34 Å, further coordination shells are included to build a cluster of 49 atoms. For this cluster, the computation includes the contributions from atoms located within the first 6 Å around Y. As shown in Figure 2 panel a, no differences are found between computations performed for clusters including contributions from atoms located within the first 5 Å (31 atoms) and 6 Å (49 atoms) around the photoabsorber. This result indicates that further coordination shells do not contribute significantly to the XANES spectrum. Therefore, we have fixed the maximum cluster size to r_{max} = 5 Å.

Once the cluster size had been fixed for the reference system we tested the performance of different exchange and correlation potentials (ECP) to account for the experimental spectrum. We have computed the Y K-edge XANES of Y(III)-triflate using both energy-dependent HL and DH ECP potentials. The imaginary part of the complex HL potential takes into account the inelastic losses of the photoelectron, although they are not accounted for when using the real DH potential. Therefore, for sake of completion, we have also performed the calculation by taking only the real part of the HL potential and, in addition, the same computation has been performed by using the energy-dependent DH by adding to it the imaginary part of the HL ECP. The results of the computations are compared to the experimental XANES spectrum in panels b and c of Figure 2. For this comparison, no convolution has been applied to the theoretical spectra.

In the case of the computation performed for the real DH or by using only the real part of the HL ECP, the computations

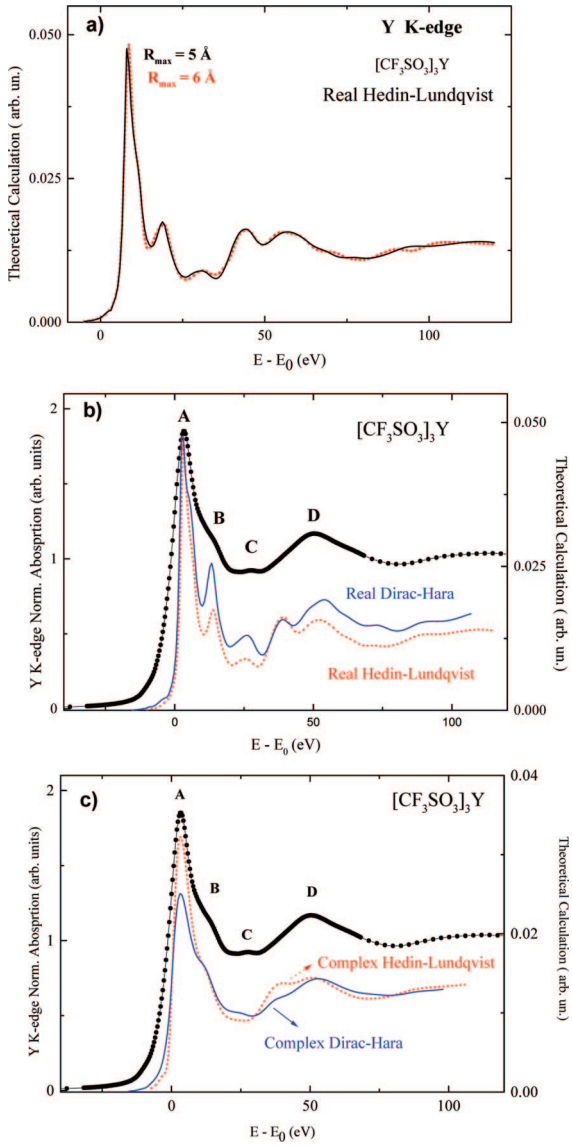

Figure 2. (a) Comparison of the theoretical spectra computed using the real part of the HL potential for Y(III)-triflate on clusters of different size covering up to $r_{max} = 5$ Å (black, solid line) and 6 Å (red, dots) around the absorbing Y atom. (b) Comparison of the experimental XANES spectrum at the Y *K*-edge of Y(III)-triflate (•) and the theoretical spectra computed for $r_{max} = 5$ Å clusters using the real HL (red, dots) and DH (blue, solid line) ECP. (c) The same comparison as in panel b is shown but using the full complex HL potential (red, dots) and the DH one with the addition of the imaginary part of the HL (blue, solid line).

reproduce satisfactorily the experimental spectral shape. The XANES spectrum of Y(III)-triflate exhibits an asymmetric main absorption line (A) with a shoulder-like feature (B) on the high-energy side. For higher energies there is a weak, but well defined, structure (C) at $E \approx 25$ eV above the edge and a strong broad peak (D) centered at $E \approx 50$ eV. All these features are well accounted for by the computations, specially regarding their relative energy separation. However, the calculated spectra show sharper resonances than the experimental ones, as expected due to the use of real potentials and the consequent neglect of inelastic excitations. It is expected that the agreement would be improved by using the complex potentials as the inelastic channels drain away amplitude from the elastic channel that carries the structural information.[20] The result of the computations performed by using both complex potentials, that is, HL and the real DH plus the imaginary part of the HL one, is shown in the lower panel of Figure 2. As expected, the use of complex potentials leads to a significant improvement of the intensity ratio between the different spectral features. However, the damping of the multiple-scattering contribution to the spectra is excessive, so that feature C is not reproduced. It should be remembered that the theoretical spectra shown in Figure 2 need to be further convoluted with a Lorentzian shape function with $\Gamma = 4$ eV to account for the core-hole lifetime and the experimental resolution.

As a final trial to optimize the computations, we have applied a self-consistent-field (SCF) procedure to build the final state potential. To achieve this, we have (SCF) stabilized a small $[YO_6]^{9-}$ cluster with an outer sphere with a +9 charge to neutralize the whole cluster. The excited final state potential was calculated by promoting one of the 1s electrons of Y to the first free energy level of the right symmetry and keeping constant the number of electrons of this state during the SCF procedure. The energy of the process is then given by the difference between the total energy of the excited final state and the initial ground state. This cluster has been embedded into the larger clusters in order to perform the MS calculations. Then, the potential of both the absorbing Y and of the six next neighbors oxygen atoms is SCF, while the potential around other atoms was built according to the Mattheis' prescription. This procedure has been previously shown to be successful on extended systems.[26−28]

The result of the SCF computation is reported in Figure 3 panels a and b for both real DH and real HL ECP. In both cases, the theoretical spectra have been convoluted with a Lorentzian shape function ($\Gamma = 4$ eV). Their comparison with the experimental spectrum of Y(III)-triflate shows that the best agreement is obtained by using the real DH potential, no matter whether the SCF or non-SCF method is used. In the case of the theoretical spectra obtained by using the real HL potential, the spectral feature C is missed in the simulation, as was the case for the non-SCF computations once the calculated spectrum has been convoluted with a Lorentzian shape function $\Gamma = 4$ eV to account for the core-hole lifetime and experimental resolution.

We have further verified these results by applying a similar procedure to the Y_2O_3 case. In Yttria (space group *I3A*-), Y occupies two different crystallographic positions Y_1 (8b) and Y_2 (24d). Consequently, the computation of the absorption cross section has to be performed separately for Y-absorbing atoms occupying both crystallographic sites. The total XANES is thus obtained as the sum of both contributions appropriately weighted according to the crystallographic occupancy (1:3). For these computations we have built a 6.5 Å cluster around the absorber. These clusters contain 73 and 76 atoms for the Y_1 (8b) and Y_2 (24d) sites, respectively. In a similar way as for Y(III)-triflate, we have also constructed SCF potentials by stabilizing a small $[YO_2]^{1-}$ cluster whose potential is embedded into the larger ones to perform the MS calculations. The results, reported in Figure 3 panels c and d, show the improved performance of the DH potential over the HL one. Moreover, the use of SCF potentials clearly improves the agreement between the computation and the experimental spectrum. In this way the computation reproduces the spectral feature C of Y(III)-triflate and, in addition, both the relative energy separation and intensity ratio of the different spectral features of both Y(III)-triflate and Y_2O_3. Finally, it is also found in this case that the use of complex potentials introduces an excessive damping of the XANES signals. In all the studied cases the addition of the imaginary part of the HL potential worsens the agreement between the experimental and calculated spectra, indicating the failure of

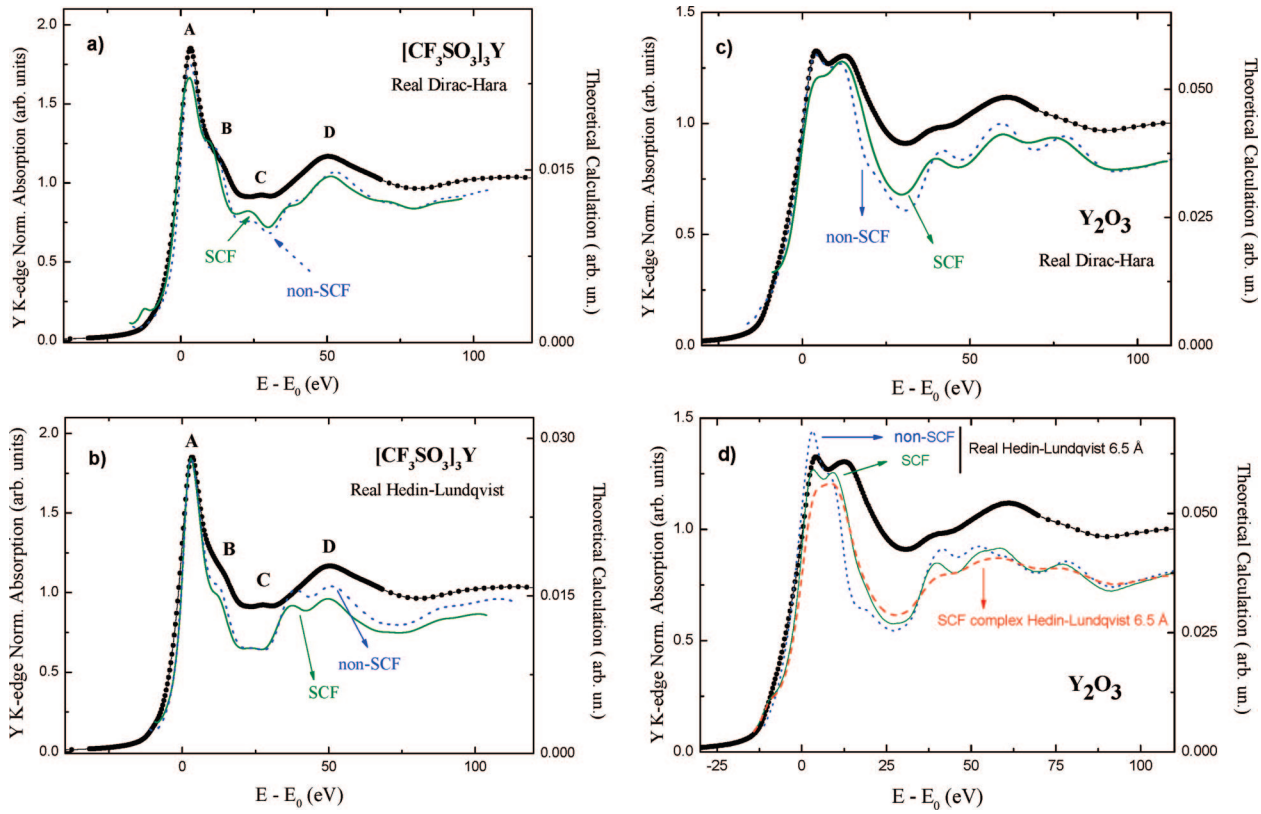

Figure 3. (a) Comparison of the experimental XANES spectrum at the Y *K*-edge of Y(III)-triflate (black, •) and the theoretical spectra computed for a 5 Å cluster using both non-SCF (blue, dotted line) and SCF (green, solid line) real DH potentials; (b) same as panel a but using real HL potentials; (c) comparison of the experimental XANES spectrum at the Y *K*-edge of Y_2O_3 (black, •) and the theoretical spectra computed for a 6.5 Å cluster using both non-SCF (blue, dotted line) and SCF (green, solid line) real DH potential. (d) same as panel c but using real HL potentials. For the sake of completeness, the SCF computation performed using the complex HL ECP is shown (red, dashed line). All the calculated theoretical spectra have been convoluted ($\Gamma = 4$ eV).[25]

the complex part of the HL ECP to account for the electron damping in these systems. In conclusion, the best agreement with the experimental data for both cases is obtained by using SCF potentials and the real DH exchange and correlation potential.

Once the main ingredients for the calculations for the yttrium solid compounds were determined, we further verified their validity by applying the parameters to the XANES calculations of yttrium complexes in solution. To this end, the XANES spectrum of the 0.5 M solution of YSCN in acetonitrile has been computed from ab initio methods. Finally, and before addressing the determination of the solvation structure of the Y(III) in DMSO solution, we have performed the computation of the XANES in its parent solid compound YDMSO,[29] the structure of which has been fully determined by XRD.[30]

In the case of the YNCS acetonitrile solution the computation was performed using a cluster of 19 atoms around the absorbing atom. This cluster includes contributions from atoms located within the first 5.2 Å around the photoabsorber: 6 N atoms at $r = 2.36$ Å, 6 C at $r = 3.5$ Å, and 6 S at 5.14 Å.[2] Calculations have been performed using the real DH ECP and also considering only the real part of the HL potential. As in the case of Y(III)-triflate, we have also used the SCF method to describe the final state potential by embedding a small $[YN_6]^{15-}$ cluster with an outer sphere with a +15 charge to neutralize the whole cluster. The results of these computations are presented in Figure 4. The experimental YNCS XANES spectrum exhibits an asymmetric main absorption line. The main absorption peak (A) lies at ~7 eV above the edge, and a shoulder-like feature (B) appears on the high-energy side at ~16 eV. For higher energies there is a broad structure (C, ~30 eV), a deep one (D) at ~42 eV above the edge, and an intense resonance (E) centered at $E \approx 60$ eV. In addition, it should be noted the existence of a weak bump at the raising edge, A_1. The computation performed using the HL potential reproduces these spectral features with the exception of the tiny feature (A_1) at the edge. However, the energy position and relative separation of the main absorption features are not well reproduced by the computation. Using DH ECP improves the result of the computation by reproducing the previously missed (A_1) feature. However, the broad resonance (E) lies at energies significantly higher than the experimental one. These problems are solved by using the self-consistency method. As shown in Figure 4, the computation performed by using the SCF potentials yields the best agreement in both relative energy separation and intensity ratio of the experimentally observed features.

In the case of the solid YDMSO, the structure used for the calculation of the XANES spectrum was determined by X-ray diffraction.[30] The structure is of very low symmetry, with a monoclinic spatial group. The computation for YDMSO has been performed by using a cluster of 27 atoms around the Y center. This cluster includes contributions from atoms located within the first 5 Å around the photoabsorber. As in the previous cases, we have investigated the most appropriate exchange and correlation potential needed for the calculations. In this way we have used both the real HL and real DH ECPs and also tested the improvements obtained by using SCF and non-SCF potentials. As shown in Figure 5, the closest match to the experimental spectrum is obtained by using the self-consistent real DH potential, as expected from the previous calculations.

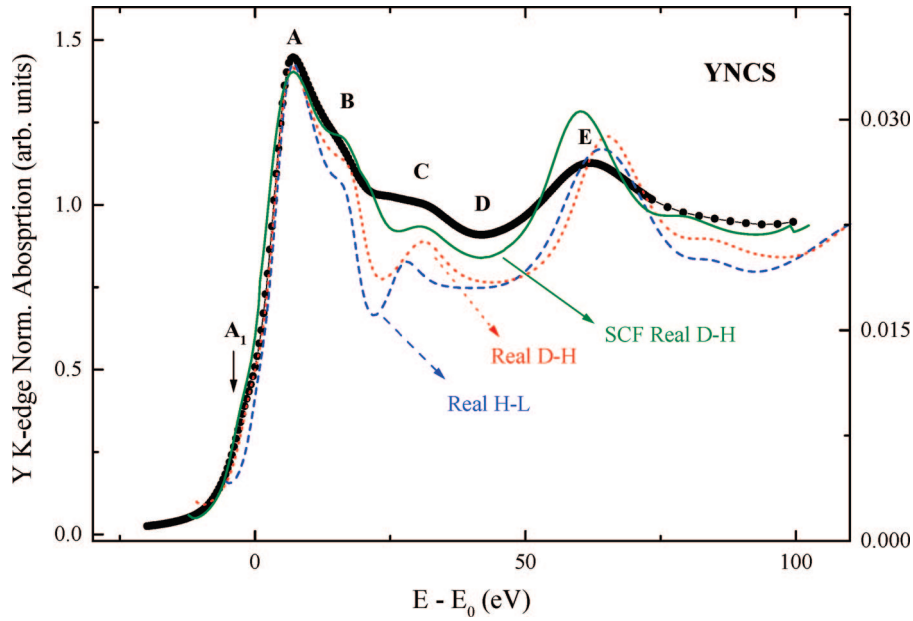

Figure 4. Comparison of the experimental XANES spectrum at the Y K-edge of YNCS (•) and the theoretical spectra computed for a 5.2 Å cluster using real HL (blue, dashed line), real DH (red, dots), and SCF real DH (green, solid line). In all the cases the theoretical spectra have been convoluted using $\Gamma = 4$ eV (see text for details).

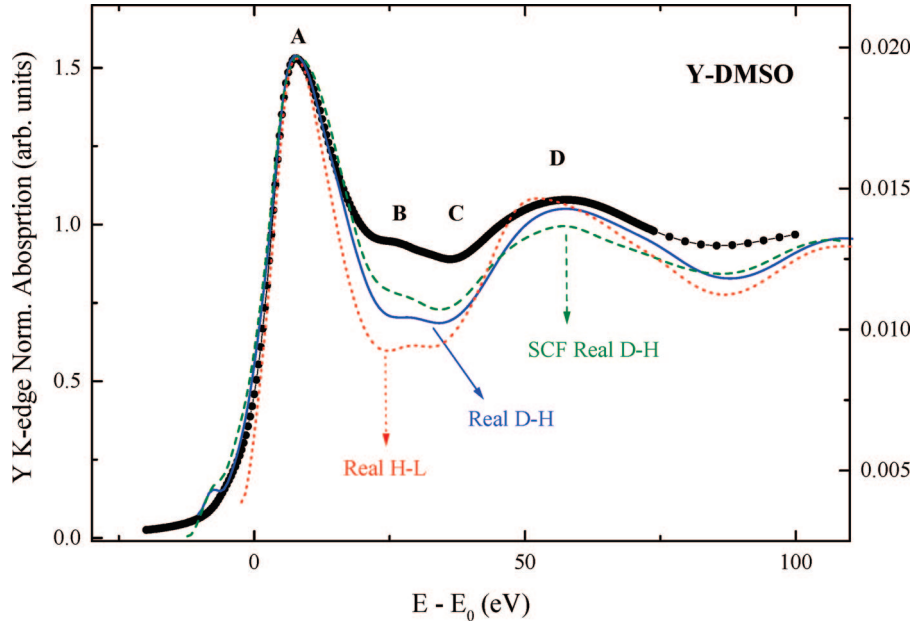

Figure 5. Comparison of the experimental XANES spectrum at the Y K-edge of YDMSO (•) and the theoretical spectra computed for a 5.2 Å cluster using real HL (red, dashed line), real DH (blue, dots), and SCF real DH (green, solid line). The theoretical spectra have been convoluted using $\Gamma = 4$ eV (see text for details).

The common result of the above calculations allows us to fix the main parameters for the simulations of the Y K-edge XANES of the 0.5 M solution of yttrium (III) in dimethyl sulfoxide. In particular, the good reproduction of the XANES spectrum of the solid solvate make us confident of the correctness of our choice to compute the XANES using the SCF real DH potential. For the computations we have used different coordination polyhedra (C6, C8, and C9), as previously explained for the EXAFS analysis.

The first coordination scheme considered is a perfectly symmetric octahedron of DMSO molecules around the yttrium center (model C6). The interatomic distances to the first and second coordination spheres formed by oxygen and sulfur atoms, respectively, were extracted from the EXAFS analysis discussed above, and the Y−O−S angle was determined by keeping the O−S distance in the DMSO as when found in the pure solvent. In a second step we have also considered a Y(III) environment in which eight DMSO molecules surround the metal, forming a distorted square antiprism (model C8). This model structure was taken from the crystal structure of $[Y(DMSO)_8]I_3$, determined by Lindqvist-Reis et al.[11] According to this study, three of the DMSO molecules are disordered with inverted conformations giving two alternative positions (A and B) for the sulfur atoms with different occupancy. The occupancy factors were refined to 0.760, 0.538, and 0.886 for the main (A) positions of the three sulfur atoms. On the basis of this, the oxygen coordination sphere was kept fixed during the computation while eight different structural arrangements in which these three sulfur

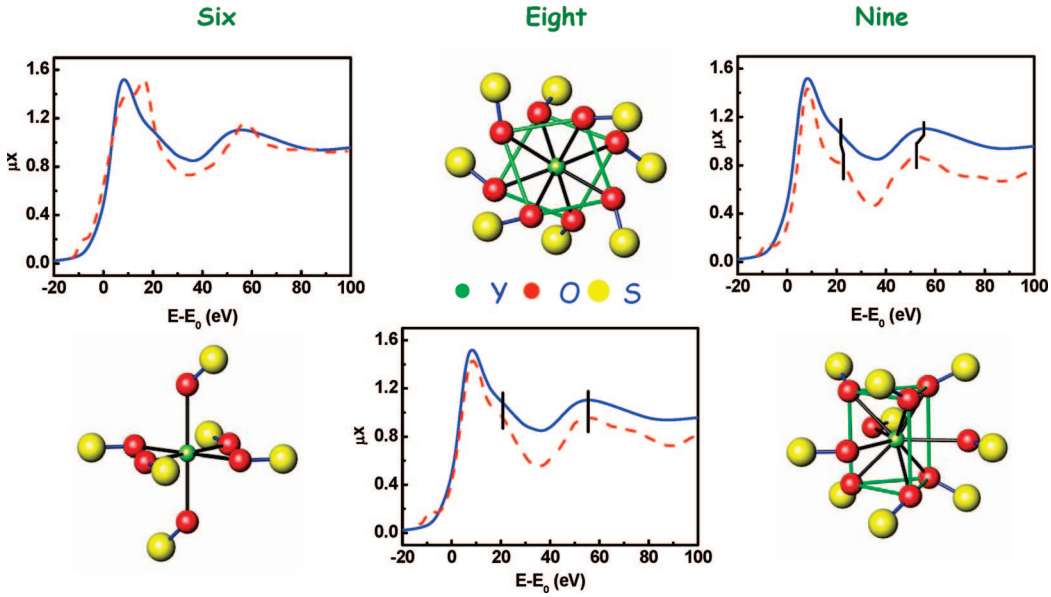

Figure 6. Comparison of the experimental XANES spectrum at the Y K-edge of a 0.5 M solution of yttrium (III) in DMSO (blue, solid line) and the theoretical computations (red, dash) performed using the SCF real DH ECP on 6- (left), 8- (center), and 9-fold (right) environments (see text for details).

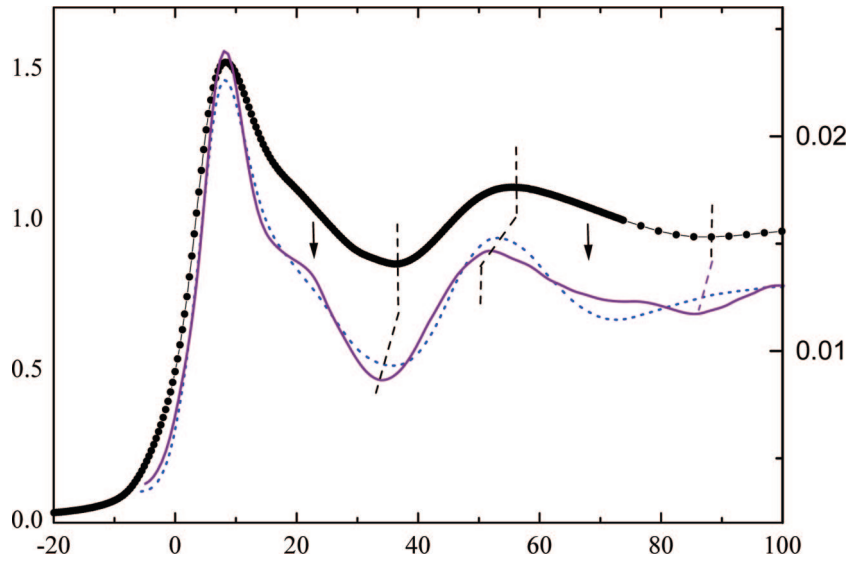

Figure 7. Comparison of the experimental XANES spectrum at the Y K-edge of a 0.5 M solution of yttrium (III) in DMSO (•) and the theoretical spectra computed for two 9-fold coordination structures: (i) (purple, solid line) tricapped trigonal prism (C9 model) and (ii) (blue, dash) a completely asymmetric structure based on the solid nitrate of the DMSO solvate (see text for details). Calculations were performed using SCF real DH ECP and further convoluted ($\Gamma = 4$ eV).

atoms are distributed over the A and B position were adopted. The computed spectra for the different structural arrangements show very few differences, although the best reproduction of the experimental spectrum was obtained by using a weighted mixture of the two extreme configurations, that is, in which the three sulfur atoms simultaneously occupy the most (AAA) and the least (BBB) probable position. Finally, a third coordination model (C9) was considered in which the yttrium center is surrounded by nine DMSO molecules, forming a tricapped trigonal prism, similar to the environment found for the yttrium hydrate in the solid triflate,[3] but with the interatomic distances being determined from the EXAFS analysis (see above). In addition, we have tested an alternative geometry for the 9-fold coordination in which a completely asymmetric structure based on the solid nitrate of the DMSO solvate was used. In this case, each of the bidentate nitrate groups were substituted by two DMSO molecules. However, the agreement of the computed spectrum with the experimental data is significantly worse than in the previous case (Figure 7).

In addition, we have also considered different Y−O−S angles, ranging between 130° and 180° (Figure 8), for each of the three coordination environments studied. Best results were obtained when a 130° Y−O−S angle was considered, in agreement with previously reported structures of trivalent cations in DMSO.[10]

The best reproduction of the experimental data obtained for each of the considered structural model are reported in Figure 6. As seen from the figure, the spectrum computed by considering six DMSO molecules surrounding the yttrium center does not reproduce all the features or relatively intensities of the experimental spectrum (see also Figure 8). In contrast, good reproduction of the experimental spectrum is obtained with both 8-fold (square antiprism) and 9-fold (tricapped trigonal prism) coordination models. It should be noted, however, that the

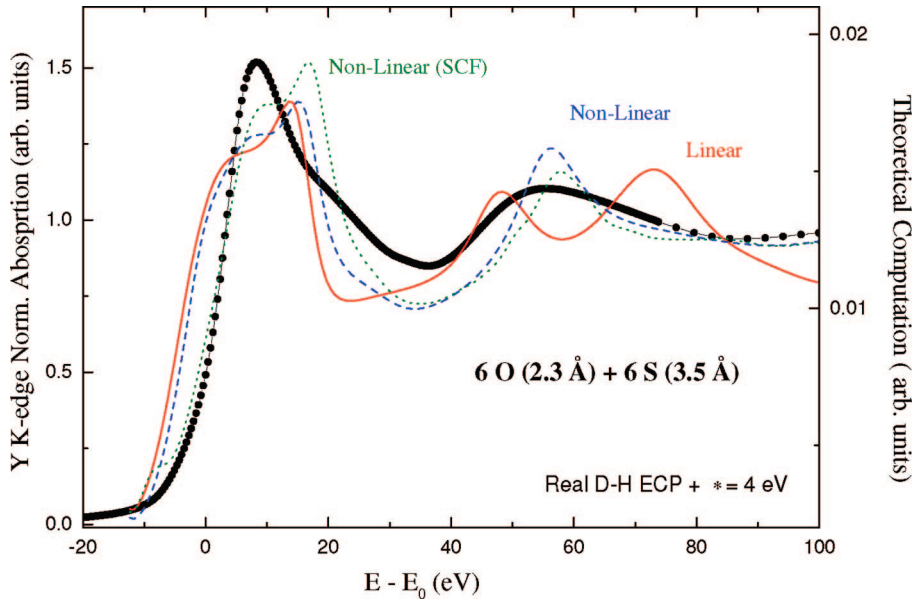

Figure 8. Comparison of the experimental XANES spectrum at the Y K-edge of a 0.5 M solution of yttrium (III) in DMSO (•) and the theoretical spectra computed on the 6-fold coordination model (C6) by considering different Y−O−S angles: 180° (red, solid line) and 130° (blue, dashed). Calculations were performed by using non-SCF DH ECP. For the sake of comparison, the computation performed for the nonlinear arrangement using a SCF potential is also shown (green, dots).

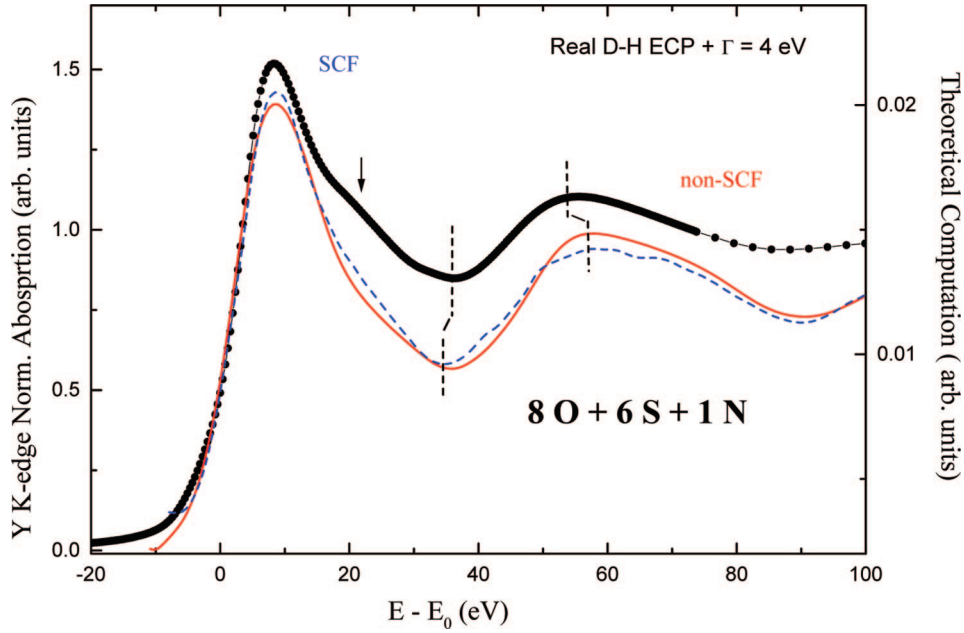

Figure 9. Comparison of the experimental XANES spectrum at the Y K-edge of a 0.5 M solution of yttrium (III) in DMSO (•) and the theoretical spectra computed for an 8-fold coordination structure based on the solid iodide salt of the yttrium DMSO solvate (see text for details). Calculations were performed using non-SCF (red, solid line) and SCF (blue, dashed) real DH ECP and further convoluted ($\Gamma = 4$ eV).

assessment of the quality of the theoretical computations is based on the correct reproduction of the shape and energy position of the different spectral features and of their relative energy separation and intensity ratio as well. Within this framework, the best reproduction of the experimental spectrum is obtained by using eight DMSO molecules around the metal center, that is, by using the distorted square antiprism model.

For the sake of completion, we have also tested the possibility of having a mixture of DMSO molecules and nitrate anions as coordinating ligands, as suggested by Johansson et al.[10] For this test, we considered in all the structural models described above that two of the DMSO molecules are substituted by a nitrate bidentate ligand. In all the cases, the theoretical reproduction of the experimental spectrum worsens. (This is shown in Figure 9 in the case of the 8-fold coordination model). Hence, we can conclude that the three nitrate anions bonded to the yttrium center in the solid compound are substituted by DMSO molecules once it is dissolved in dry DMSO, in agreement with previous studies.[9]

Summary and Conclusions

In this work we have studied the solvation structure of yttrium (III) prepared by dissolving the nitrate salt of the solvate in anhydrous DMSO by combining both EXAFS and XANES techniques. The EXAFS analysis is not conclusive regarding the different coordination polyhedra of the solvent structure of yttrium (III) in DMSO. Therefore, we have performed an Y

K-edge XANES study by comparing the experimental XANES spectrum to theoretical computations performed within the multiple-scattering framework. The XANES computations have been performed for different Y(III) model compounds in order to optimize several computational details intending to furnish the best agreement, both in energy and intensity, between the experimental and theoretical XANES spectral features. The best agreement with the experimental data is obtained by using SCF potentials and the real DH exchange and correlation potential.

These results have been transferred to the analysis of the solution sample, and several possible coordination environments and conformations of the DMSO molecule have been investigated, including a regular octahedral arrangement, an 8-fold distorted square antiprism, and a 9-fold tricapped trigonal prism. Our results indicate that the solvation sphere of the yttrium cation is best modeled by eight DMSO molecules forming a distorted square antiprism with the Y−O−S angle close to 130°.

This study has shown the capabilities and limitations of the EXAFS technique and in which manner these limitations can be overcome using the information contained in the XANES region. These results illustrate how the high sensitivity of the near-edge part of the absorption spectrum to the bonding geometry makes XANES an incomparable stereochemical probe, and that the combined analysis of both EXAFS and XANES regions is particularly appropriate to gather information about the Y coordination in these systems.

Acknowledgment. This work was partially supported by the Spanish CICYT Research Projects No. MAT2005-06806-C04-04 and No. MAT2008-06542-C04-01 and the FEDER program.

References and Notes

(1) Martin, J. L.; Thompson, L. C.; J.Radonovich, L.; Glick, M. D. *J. Am. Chem. Soc.* **1968**, *90*, 4493.

(2) Díaz-Moreno, S.; Martínez, J. M.; noz Páez, A. M.; Sakane, H.; Watanabe, I. *J. Phys. Chem.* **1998**, *102*, 7435.

(3) Harrowfield, J. M.; Kepert, D. L.; Patrick, J. M.; White, A. H. *Aust. J. Chem.* **1983**, *36*, 483.

(4) Cotton, F. A.; Davison, A.; Day, V. W.; Fredich, M. F.; C., C. O.; Swanson, R *Inorg. Chem.* **1982**, *21*, 1211.

(5) Bukowska-Strzyzewska, M.; Tosic, A. *Acta Crystallogr. B* **1982**, *38*, 950.

(6) Bell, A. M.; Smith, A. J. *Acta Crystallogr. C* **1990**, *46*, 960.

(7) Pisaiello, D. L.; Nichols, P. J.; Ducommun, Y.; Merbach, A. E. *Helv. Chim. Acta* **1982**, *65*, 1025.

(8) Díaz-Moreno, S.; Munoz-Páez, A.; Chaboy, J. *J. Phys. Chem. A* **2000**, *104*, 1278.

(9) Ramalingam, S. K.; Soundararajan, S. *J. Inorg. Nucl. Chem.* **1967**, *29*, 1763.

(10) Johansson, G.; Yokoyama, H.; Ohtaki, H. *J. Sol. Chem.* **1991**, *20*, 859.

(11) Lindqvist-Reis, P.; Näslund, J.; Persson, I.; Sandström, M. *J. Chem. Soc., Dalton Trans.* **2000**, 2703.

(12) *X-Ray Absorption: Principles, Applications, Techniques of EXAFS, SEXAFS, XANES*; R., P., D., K., Eds.; J. Wiley & Sons: New York, 1988.

(13) Munoz-Páez, A.; Gil, M.; Martinez, J. M.; Sánchez-Marcos, E. *Physica B* **1995**, *241*, 208.

(14) Ravel, B.; Newville, M. *J. Synch. Rad.* **2005**, *12*, 537.

(15) J, J.; Rehr, S. I. Z.; Albers, R. C *Phys. Rev. Lett.* **1992**, *69*, 3397.

(16) Newville, M. *J. Synch. Rad.* **2001**, *8*, 322.

(17) Benfatto, M.; Natoli, C. R.; Bianconi, A.; García, J.; Marcelli, A.; Fanfoni, M.; Davoli, I. *Phys. Rev. Lett.* **1986**, *34*, 5774.

(18) Natoli, C. R.; Benfatto, M. *J. Phys. Paris. Colloq.* **1986**, *47*, C8–11.

(19) Lee, P. A.; J.B., P. *Phys. Rev. B* **1975**, *11*, 2795.

(20) Natoli, C. R.; Benfatto, M.; Longa, S. D.; Hatada, K. *J. Synch. Rad.* **2003**, *10*, 26.

(21) Chaboy, J.; Quarteri, S. *Phys. Rev. B* **1995**, *52*, 6349.

(22) Mattheis, L. F. *Phys. Rev. A* **1964**, *133*, 1399.

(23) Norman, J. G. *Mol. Phys.* **1974**, *81*, 1191.

(24) Clementi, E.; Roetti, C. *Atomic Data Nucl. Data Tables* **1974**, *14*, 1974.

(25) Krause, M. O.; Oliver, J. H. *J. Phys. Chem. Ref. Data* **1979**, *8*, 329.

(26) Chaboy, J.; Benfatto, M.; Davoli, I. *Phys. Rev. B* **1995**, *52*, 10014.

(27) Wu, Z.; Benfatto, M.; Natoli, C. R. *Phys. Rev. B* **1992**, *45*, 51.

(28) Pedio, M.; Benfatto, M.; Aminpirooz, S.; Haase, J. *Phys. Rev. B* **1994**, *50*, 6596.

(29) Chaboy, J.; Munoz-Páez, A.; Díaz-Moreno, S. *Chem.—Eur. J.* **2001**, *7*, 1102.

(30) Antsyshkina, A. S.; Sadikov, G. G.; Rodnikova, M. N.; Mikhailicjenko, A. I.; Baklykova, T. V. *Russ. J. Inorg. Chem.* **2002**, *47*, 367.

JP809575G